 doi:10.20944/preprints202012.0028.v1

Article

Flow Cytometric Methods for the Detection of Intracellular Signaling Proteins and Transcription Factors Reveal Heterogeneity in Differentiating Human B Cell Subsets

Casper Marsman[1], Tineke Jorritsma[1], Anja ten Brinke[1], and S. Marieke van Ham[1,2] *

[1] Department of Immunopathology, Sanquin Research and Landsteiner Laboratory, Amsterdam UMC, University of Amsterdam, Amsterdam, The Netherlands.
c.marsman@sanquin.nl (C.M), t.jorritsma@sanquin.nl (T.J), a.tenbrinke@sanquin.nl (A.t.B), m.vanham@sanquin.nl (S.M.v.H)

[2] Swammerdam Institute for Life Sciences, University of Amsterdam, Amsterdam, the Netherlands.

* Correspondence: m.vanham@sanquin.nl; Tel: +31-(0)20-512 3158

Abstract: Flow cytometric detection of intracellular (IC) signaling proteins and transcription factors (TFs) will help elucidate the regulation of B cell survival, proliferation and differentiation. However, simultaneous detection of signaling proteins or TFs, with membrane markers (MM) can be challenging as required fixation and permeabilization procedures can affect functionality of conjugated antibodies. Here, a phosphoflow method is presented for detection of activated NF-κB p65 and phosphorylated STAT1, STAT3, STAT5 and STAT6 together with B cell differentiation MM CD19, CD27 and CD38. Additionally, a TF-flow method is presented that allows detection of B cell TFs; PAX5, c-MYC, BCL6, AID and antibody-secreting cell (ASC) TFs BLIMP1 and XBP-1s together with MM. Applying these methods on *in vitro* induced human B cell differentiation cultures showed significantly different steady-state levels, and responses to stimulation, of phosphorylated signaling proteins in CD27-expressing B cell and ASC populations. The TF-flow protocol and UMAP analysis revealed heterogeneity in TF-expression within stimulated CD27 or CD38-expressing B cell subsets. The methods presented here allow for sensitive analysis of STAT and NF-κB p65 signaling and TFs together with B cell differentiation MM at single-cell resolution. This will aid further investigation of B cell responses in both health and disease.

Keywords: Differentiation, germinal center, antibody-secreting cells, phosphorylated STATs, NF-κB1

1. Introduction

One of the cornerstones of the adaptive immune system is the ability of B cells to respond to pathogens and differentiate into antibody-secreting cells. The generation of antibody-secreting cells (ASCs) is mainly regulated by follicular T helper cells [1, 2] (T_{FH}) within germinal centers [3] (GCs) and are crucial for the development of high affinity antibodies [4, 5]. B cells are activated upon antigen recognition by the B cell receptor (BCR). Subsequently the antigen is internalized and presented on MHC-II in order to form a cognate interaction with the T_{FH} cell[6]. This interaction provides multiple stimuli indispensable for GC B cell proliferation and differentiation, such as membrane-bound CD40L that activates CD40 on the B cell [7, 8] and the T_{FH} hallmark cytokine IL-21 that binds to the IL-21 receptor [9–11]. Furthermore, T_{FH} cells are also able to produce IL-4 [12, 13] which contributes to class-switching and proper GC formation in combination with IL-21 [14–16]. When CD40L binds CD40 on the B cell surface, it induces activation of NF-κB p65 (canonical, heterodimerizes with NF-κB1) and NF-κB p52 (non-canonical, also known as NF-κB2) pathways [17–19]. The secreted cytokines IL-4 and IL-21 bind to their respective receptors and induce JAK-STAT pathways. IL-4

 doi:10.20944/preprints202012.0028.v1

induces phosphorylation of STAT6[20]–[22] whereas IL-21 mainly induces phosphorylation of STAT1, STAT3 and, to a lesser extent, STAT5[22], [23]. After phosphorylation events, these signaling proteins translocate to the nucleus where they can regulate transcription [24, 25]. The induction of both NF-κB and STAT pathways are essential as mutations in involved genes are known to cause primary immunodeficiencies [10, 26].

Regulation of transcription factors (TFs) in B cell and GC responses is highly complex and dynamic [27–29]. B cell identity is maintained by high expression of PAX5 [30]. After stimulation by T cells, the GC is formed and BCL6 and AID expression is upregulated in B cells [31]. Within the GC, c-MYC is crucial for maintenance of the GC by regulating division capacity and cycling of GC B cells [32–34]. Differentiation into ASCs requires downregulation of PAX5, BCL6, AID and c-MYC and upregulation of BLIMP1 and XBP-1 [35, 36]. Additionally, XBP-1 transcripts are alternatively spliced into XBP-1s transcripts for efficient functioning of the unfolded-protein response [33, 37]. As the GC response and differentiation process is highly dynamic, a range of TFs have to be simultaneously measured with currently known membrane markers (MM) to allow further investigation of heterogeneity in these responses and to further investigate the effect of stimulatory signals on the expression of these TFs.

The regulation of TF-expression through intracellular signal transduction pathways activated by TFH-cell provided CD40L, IL-21 and IL-4 are essential to the GC response and B cell differentiation. The ability to monitor both this signaling and transcriptional regulation is necessary to enable fundamental research on wanted B cell responses against pathogens and unwanted B cell responses as observed in autoimmune diseases [38–40] or during allo-antibody formation after blood transfusion [41]. Additionally, transcriptional dysregulation and overactivated signaling pathways can lead to B cell malignancies [42, 43]. Finally, it can aid in the development and characterization of therapeutic inhibitors for a range of diseases [44].

Recently it was elegantly shown that detection of BCR signaling by flow cytometry has a clear advantage over the detection of the BCR downstream signaling molecules by western blot [45]. The authors clearly show that phosphoflow analysis allows for a precise detection of BCR signaling at a single-cell resolution in a range of human and mouse B cell subsets. The next steps to study or target B cell differentiation in health and disease is combining detection of NF-κB and p-STAT signaling pathways activated by TFH signals, with MM analysis, to elucidate crosstalk between BCR, CD40 and cytokine receptors. Detection of both MM and IC phospho-proteins has been optimized for analysis in murine lymphoid cells[46]. However, an optimized method for simultaneous analysis of both MM and signaling in specific human B cell subsets undergoing differentiation is still highly desired. Furthermore, detection of crucial TFs with MM expression during T-dependent stimulation of B cells will also allow further elucidation of human B cell differentiation.

Here we present two methods, one that allows monitoring of signaling via STAT molecules and NF-κB and one that allows for the detection of TFs dynamically expressed throughout *in vitro* T-cell dependent B cell differentiation. Both methods allow for sample processing in a 96-wells format and allow for analysis at the level of individual B cells in distinct B cell subpopulations, revealing a previously unappreciated heterogeneity in stimulated B cell subpopulations.

2. Materials and Methods

2.1. Cell lines

NIH3T3 fibroblasts expressing human CD40L (3T3-CD40L$^+$)[47] were cultured in IMDM (Lonza) containing 10% FCS (Serana), 100 U/ml penicillin (Invitrogen), 100 µg/ml streptomycin (Invitrogen), 2mM L-glutamine (Invitrogen), 50 µM β-mercaptoethanol (Sigma Aldrich) and 500 µg/ml G418 (Life Technologies).

2.2. Isolation of peripheral blood mononucleated cells and B cells from human healthy donors

 doi:10.20944/preprints202012.0028.v1

Buffy coats of healthy human donors were obtained from Sanquin Blood Supply. All healthy donors provided written informed consent in accordance with the protocol of the local institutional review board, the Medical Ethics Committee of Sanquin Blood Supply, and conforms to the principles of the Declaration of Helsinki. Peripheral blood mononucleated cells (PBMCs) were isolated from buffy coats using a Lymphoprep (Axis-Shield PoC AS) density gradient. Afterwards, $CD19^+$ B cells were isolated using magnetic Dynabeads (Invitrogen) and DETACHaBEAD (Invitrogen) according to manufacturer's instructions.

2.3. In vitro B cell stimulation cultures

3T3 -$CD40L^+$ were harvested, irradiated with 30 Gy and seeded in B cell medium (RPMI 1640 (Gibco) without phenol red containing 5% FCS, 100 U/ml penicillin, 100 µg/ml streptomycin, 2mM L-glutamine, 50 µM β-mercaptoethanol and 20 µg/ml human apo-transferrin (Sigma Aldrich; depleted for human IgG with protein G sepharose (GE Healthcare)) on 96-well flat-bottom plates (Nunc) to allow adherence overnight. 3T3 -$CD40L^+$ were seeded at 10.000 cells per 96-well. The next day, $CD19^+$ B cells were thawed from cryo-storage and washed with B cell medium. B cells were rested at 37°C for 1 h before counting. 5000 or 10.000 $CD19^+$ B cells were co-cultured with the irradiated 3T3-$CD40L^+$ fibroblast in the presence of $F(ab')_2$ fragment Goat Anti-Human IgA/G/M (5 µg/ml; Jackson Immunoresearch), IL-4 (25 ng/ml; Cellgenix) and IL-21 (50 ng/ml; Peprotech) for up to six days. The B cell suspension, 3T3-$CD40L^+$ plates and stimulation mix were all heated to 37°C before mixing components together. After adding the B cells to the well the plate was centrifuged for 1 min at 400x*g* to force all B cells onto the 3T3-$CD40L^+$ layer.

2.4. Phosphoflow protocol

2.4.1. Flow cytometry antibodies

Antibodies used here were first titrated and validated. This was done by using either the manufacturers advised positive controls or by using a known strong stimulus found in literature[48], [49]. During the validation and titration samples were compared to unstimulated and unstained controls. As conditions and flow cytometer settings differ per lab it is advised that these dilutions are taken as guidelines and that these are validated within each individual lab (Table 1).

2.4.2. Harvesting, fixation and permeabilization

At indicated timepoints wells were resuspended with a multichannel and transferred to 96-well V-bottom plates (Nunc). Multiple culture wells were pooled, up to a full 96-well plate per replicate. After harvest cells were kept on ice or at 4°C at all times. Cells were washed with 150 µl ice-cold PBS/0.1% bovine serum albumin (BSA; Sigma Aldrich), centrifuged at 600x*g* for 2 minutes and pooled. Samples were stained in a 25 µl staining mix with 1:1000 LIVE/DEAD Fixable Near-IR Dead cell stain kit (Invitrogen) and anti-CD19 and -CD38 antibodies (Table 1.) diluted in ice-cold PBS/0.1% BSA for 15 minutes on ice. Samples were washed once with 150 µl ice-cold PBS/0.1% BSA, centrifuged at 600x*g* for 2 minutes and fixed with 37°C 4% paraformaldehyde (PFA; Sigma) for 10 minutes at 37°C. After fixation, samples were centrifuged at 600x*g* for 2 minutes, washed once with 150 µl ice-cold PBS/0.1% BSA and permeabilized with 90% methanol from -20°C freezer. Samples were incubated for at least 30 minutes or stored at -20°C till day of FACS analysis.

2.4.3. Intracellular stain and FACS analysis

After permeabilization, samples were centrifuged at 600x*g* for 2 minutes followed by two consecutive washes with 150 µl ice-cold PBS/0.1% BSA. Samples were then stained in 25 µl staining mix containing anti-CD27, anti-NF-κBNF-κB p65, anti-p-STAT1, anti-p-STAT3, anti-p-STAT5 and

 doi:10.20944/preprints202012.0028.v1

anti-p-STAT6 (Table 1) diluted in PBS/0.1% BSA. Samples were incubated for 30 minutes on a plate shaker at room temperature. Samples were washed twice with 150 µl PBS/0.1%BSA. Finally, samples were resuspended in a volume of 150 µl and of which 100 µl was measured on a flow cytometer. The flow cytometer was calibrated by compensating for all conjugates using UltraComp eBeads compensation beads (Invitrogen). All measurements were performed on a BD FACSymphony machine and analyzed using FlowJo Software v10.6.2 (Treestar).

2.5 Real-time semi-quantitative RT-PCR

Different B cell subsets (as indicated) were sorted on FACSAriaIII. After sorting, RT-PCR was performed as described before [50]. Briefly, cells were lysed in peqGOLD Trifast (PeQlab) and GlycoBlue (Ambion) was added as a carrier. Total RNA was extracted according to the manufacturer's instructions. First strand cDNA was reverse transcribed using random primers (Invitrogen) and SuperScript™ II Reverse Transcriptase (Invitrogen) according to the manufacturer's instructions. Primers were developed to span exon-intron junctions and then validated. Gene expression levels were measured in duplicate reactions for each sample in StepOnePlus (Applied Biosystems) using the SYBR green method with Power SYBR green (Applied Biosystems). Primers sets used were as followed:

c-MYC: F: 5'-TACAACACCCGAGCAAGGAC-3'
R: 5'GAGGCTGCTGGTTTTCCACT-3'

Published previously [23]:
PA5: F: 5'-ACGCTGACAGGGATGGTG-3',
R: 5'-CCTCCAGGAGTCGTTGTACG-3'.

BCL6: F: 5'-GAGCTCTGTTGATTCTTAGAACTGG-3';
R: 5'-GCCTTGCTTCACAGTCCAA-3'

BLIMP1: F: 5' -AACGTGTGGGTACGACCTTG-3',
R: 5'-ATTTTCATGGTCCCCTTGGT-3'

XBP-1: F: 5'-CCGCAGCACTCAGACTACG-3',
R: 5'-TGCCCAACAGGATATCAGACT-3'

AICDA: F: 5'-GACTTTGGTTATCTTCGCAATAAGA-3',
R: 5'AGGTCCCAGTCCGAGATGTA-3'

Expression was normalized to the internal control of 18S rRNA [50]:
18S-rRNA: F: 5'-CGGCTACCACATCCAAGGAA-3',
R: 5'-GCTGGAATTACCGCGGCT-3'

2.6. TF – flow protocol

Cells were harvested, pooled and pelleted before washing twice with 10 ml PBS/0.1% BSA. Samples were counted and $1*10^6$ were added per well to a 96-well V-bottom plate. Samples were centrifuged at 600x*g* for 2 minutes and stained with 25 µl staining mix with 1:1000 LIVE/DEAD Fixable Near-IR Dead cell stain kit, anti-CD19, anti-CD27 and anti-CD38 antibodies (Table 1) and incubated for 15 minutes in the fridge. Samples were washed once with 150 µl ice-cold PBS/0.1% and centrifuged at 600x*g* for 2 minutes. Samples were then fixated with 100 µl Foxp3 fixation buffer (eBioscience) for 30 minutes in the fridge. Next, 150 µl Foxp3 permeabilization buffer (eBioscience) was added and samples were centrifuged at 600x*g* for 2 minutes. After removing the supernatant,

 doi:10.20944/preprints202012.0028.v1

samples were stained with 25 µl staining mix containing anti-PAX5, anti-BCL6 and either anti-c-MYC, anti-BLIMP1, anti-XBP-1s or anti-AID (Table 1) diluted in Foxp3 permeabilization buffer and incubated for 30 minutes in the fridge. Samples were washed with 150 µl Foxp3 permeabilization buffer. Finally, samples were resuspended in a volume of 140 µl and of which 90 µl was measured on a flow cytometer. The flow cytometer was calibrated by compensating for all conjugates using UltraComp eBeads compensation beads (Invitrogen). All measurements were performed on a BD FACSymphony machine and analyzed using FlowJo Software v10.6.2 (Treestar).

2.7. Multimarker analysis using UMAP

Live $CD19^+$ B cells were gated on and duplicates from three donors were randomly down-sampled to 10.000 events and subsequently concatenated into a single 60.000 event FCS file using the DownSample plugin in FlowJo v10.6.2. Next, the concatenated sample was analyzed using the Uniform Manifold Approximation and Projection (UMAP) plugin v3.1 in FlowJo v10.6.2. UMAP is a machine learning algorithm used for dimensionality reduction to visualize high parameter datasets in a two-dimensional space. UMAP plugin settings were as followed: Distance function Euclidean; number of neighbors 30; minimal distance 0.5 and number of components 2. The UMAP dot plot generated can be manipulated as a standard dot plot and allows for multiple parameter and heatmap overlays in the FlowJo layout-editor. The DownSample and UMAP FlowJo plugins can be found on the FlowJo Exchange website.

2.8. Statistical analysis

Statistical analysis was performed using GraphPad Prism (version 8; GraphPad Software). Phosphoflow data was analyzed with mixed-effects analysis with Tukey's multiple comparison test. TF mRNA and flow data were analyzed with repeated-measures ANOVA with Tukey's multiple comparison test. Results were considered significant at $p<0.05$. Significance was depicted as * $p < 0.05$, ** $p < 0.01$, **** $p < 0.0001$.

3. Results

3.1. In vitro stimulation of B cells

An *in vitro* stimulation system that mimics a T-cell dependent B cell stimulation (Fig. 1A) was used to functionally asses the NF-κB and STAT signaling and TF profiles during B cell differentiation within specific B cell and ASC subpopulations. In this culture system $F(ab)_2$ fragments targeting IgM, IgG and IgA were used to induce BCR signaling. Irradiated human-CD40L expressing 3T3-fibroblasts were used to mimic the T_{FH}-mediated CD40 co-stimulation essential for B cell differentiation. Additionally, recombinant cytokines IL-21 and IL-4 were added to induce IL-21R and IL-4R signaling. B cells were cultured for up to 6 days and B cell differentiation was assessed based on the relative expression CD27 and CD38 (Fig. 1B, full gating strategy in Suppl. Fig. 1).. Relative expression of CD27 and CD38 (Fig. 1C-D) demonstrated significant B cell differentiation into the $CD27^+CD38^+$ ASC-population started after 96 hours and increased over time.

Preprints (www.preprints.org) | NOT PEER-REVIEWED | Posted: 2 December 2020 doi:10.20944/preprints202012.0028.v1

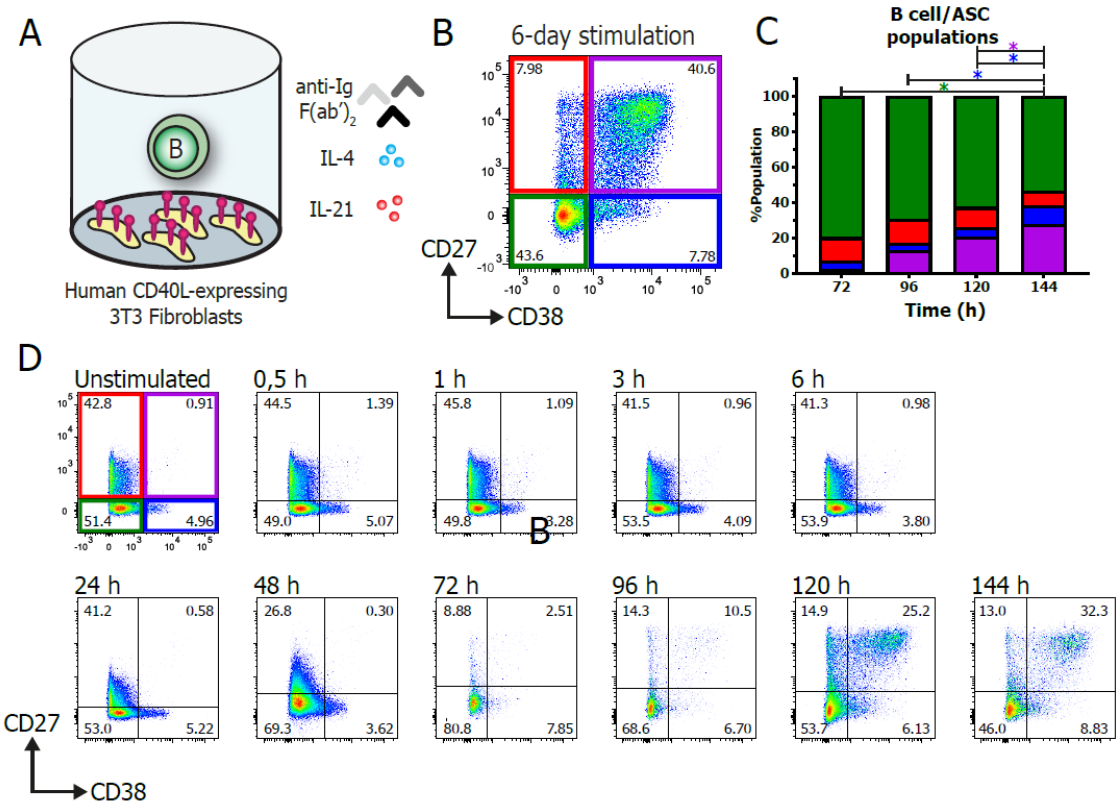

Figure 1. Efficient *in vitro* generation of human B cell and antibody-secreting cell subpopulations. Total human B cells (n=3) were stimulated *in vitro* to generate multiple B cell and antibody-secreting cell (ASC) subpopulations. **(A)** Schematic overview of the culture system used to induce B cell differentiation. 5000 $CD19^+$ human B cells were stimulated with a human-CD40L expressing 3T3 feeder layer, an anti-Ig $F(ab)_2$ mix (5 ug/ml) targeting IgM, IgG and IgA, and recombinant cytokines IL-4 (25 ng/ml) and IL-21 (50 ng/ml). **(B)** Representative FACS plot after 6 days of culture based on expression of CD27 and CD38. **(C)** Quantification of the relative percentage of CD27 and CD38 subpopulations in the total $CD19^+$ B cell population between 3 and 6 days of culture. N=4, P values were calculated by 2-way ANOVA with Tukey's multiple comparison test, * $p < 0.05$. **(D)** Representative FACS plots of a time course experiment of B cell differentiation dynamics of one B cell donor, as measured over the course of 6 days culture

3.2. Establishment of phosphoflow assay shows differences in 6hosphor-signaling profiles within B cell subpopulations

To be able to investigate the dynamics of STAT and NF-κB signaling during B cell differentiation a phosphoflow protocol and panel were designed to allow simultaneous detection of differentiation MM together with intracellular signaling via p-STAT and activated NF-κB p65. Validation and titration of conjugated antibodies used here are listed in Table 1. Several antibodies directed against MMs for B cell differentiation and their conjugated fluorophores were tested for compatibility with the PFA-based fixation and methanol-based permeabilization protocol. Violet fluorophores like BV510 and V450, together with FITC and APC fluorophores survived permeabilization with only a slight loss in fluorescence (Suppl. Fig 2). Additionally, the anti-CD27 clone L128 was found to stain cells efficiently even after fixation and permeabilization. Even though some stains were significantly less after permeabilization or showed a significantly lower MFI, CD19, CD27 and CD38 populations were still easily distinguished. These antibodies and fluorophore properties combined allowed for an extensive panel to stain both MM and IC signaling proteins using the protocol presented here.

Preprints (www.preprints.org) | NOT PEER-REVIEWED | Posted: 2 December 2020 doi:10.20944/preprints202012.0028.v1

Table 1. Antibodies used for phospho- and transcription factor- flow cytometry

Antibody Target	Conjugate	Clone	Manufacturer	Dilutions*	Cat. No.
Membrane Markers					
CD19	APC	SJ25C1	BD	1:400	345791
	BV510	SJ25C1	BD	1:100	562947
CD27	APC	L128	BD	1:50	337169
	PE	L128	BD	1:50	340425
	BUV395	L128	BD	1:100	563815
	BUV737	L128	BD	1:100	612829
CD38	V450	HB7	BD	1:100	646851
	FITC	T16	Beckman Coulter	1:50	A07778
Phosphoflow					
pSTAT1	Percp-Cy5.5	4a pY701	BD	1:5	560113
pSTAT3	PE	4/P-STAT3	BD	1:5	612569
pSTAT5	Pacific Blue	47/Stat5 (pY694)	BD	1:5	560311
pSTAT6	AF647	18/P-Stat6	BD	1:5	612601
NF-κB p65	PE-Cy7	K10-895.12.50	BD	1:25	560335
Transcription Factors					
PAX5	PE	1H9	Biolegend	1:10.000	649708
c-MYC	AF647	D84C12	CST	1:150	13871S
BCL6	PE-Cy7	7D1	Biolegend	1:400	358512
BLIMP1	AF647	#646702	R&D	1:40	IC36081R-025
XBP-1s	AF647	Q3-695	BD	1:40	562821
AID	AF647	EK2-5G9	BD	1:150	565785

*Optimal antibody dilutions as defined for the method and staining procedure used in this paper. As staining conditions and flow cytometer settings may differ per lab it is advised that these dilutions are taken as guidelines and that these are validated within each individual lab. See M&M for the full staining procedure.

For detection of p-STAT and activated NF-κB signaling, B cells were stimulated as above. $CD19^+$ and CD27/CD38 subpopulations were gated (Fig 2A) and analyzed for expression of p-STAT1, p-STAT3, p-STAT5, p-STAT6 and activated NF-κB p65. Analysis of p-STAT1 per CD27/CD38 subpopulation showed clear induction of STAT1 signaling in all populations over time, with the $CD27^+CD38^+$ ASC population reaching its maximum pSTAT1 value around 48 hours. In contrast, pSTAT1 peaked at 72 hours in the three B cell populations, with higher and more sustained p-STAT1 levels in the $CD27^-CD38^+$ population.(Fig 2B).

p-STAT3 levels increased over time with a peak at 72 hours of stimulation (Fig 2C). There were significant differences between subpopulations with a tendency of higher phosphorylation of STAT3 in the $CD27^-CD38^-$ population.

p-STAT6 levels in the B cell subpopulations were significantly different at start of the culture up until 6 hours of stimulation (Fig 2D). p-STAT6 increased in all subpopulations until 48 hours after stimulation. After this peak, , the $CD27^-CD38^-$ and $CD27^-CD38^+$ populations remained higher and showed more sustained phosphorylation of STAT6 compared to the other populations.

NF-κB p65 was activated already after 30 minutes of stimulation followed by a second and higher peak of activation at 48 – 72 hours of stimulation. (Fig 2E). To accommodate differences in fluorescence intensity between donors (Suppl. Fig 4A)., the fold change of NF-κB p65 was plotted to compare the dynamics of NF-κB p65 activation over time between the subpopulations. After 72 hours of stimulation NF-κB p65 levels declined in all subpopulations. There was a tendency of higher and more sustained NF-κB p65 activation in the $CD27^-CD38^-$ and $CD27^-CD38^+$ populations. The significant differences between pSTAT and NF-κB p65 levels in the CD27/CD38 subpopulations could not be attributed to differences in cell size (Suppl. Fig. 5A-B). Altogether, analysis showed that this panel can be used to study dynamics of the combined pSTAT and NF-κB p65 signaling cascades during B cell to ASC differentiation.

Preprints (www.preprints.org) | NOT PEER-REVIEWED | Posted: 2 December 2020 doi:10.20944/preprints202012.0028.v1

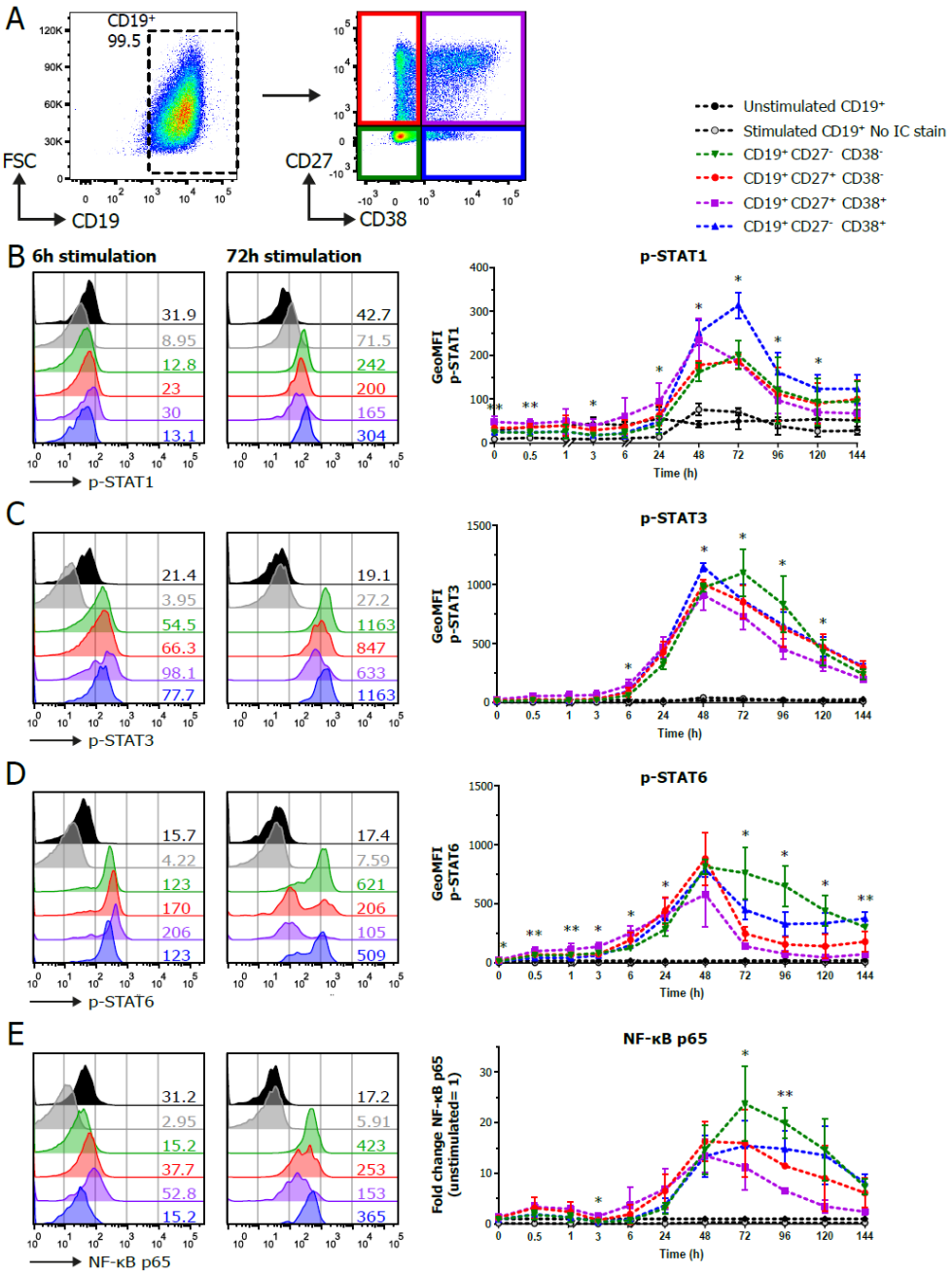

Figure 2. Phosphoflow analysis of stimulated human B cells show differences between CD27/CD38 subpopulations. Human B cells (n=3-4) were stimulated with human-CD40L expressing 3T3 feeder layer, an anti-Ig F(ab)$_2$ mix (5 ug/ml) targeting IgM/IgG/IgA and recombinant cytokines IL-4 (25 ng/ml) and IL-21 (50 ng/ml) and multiple signaling proteins were analyzed by phosphoflow analysis over the course of 6-day culture. **(A)** Representative FACS plots show the gating strategy of CD19$^+$ and CD27/CD38 subpopulations by phosphoflow analysis after 96h stimulation. **(B-E)** Representative histogram overlays of p-STAT1 **(B)**, p-STAT3 **(C)**, p-STAT6 **(D)** or NF-κB p65 **(E)** staining in unstimulated and stimulated CD19$^+$ and CD27/CD38 subpopulations after 6 h and 72 h stimulation (left) and the quantification of GeoMFI within the different subpopulations over the course of 6 days culture (right). Values depicted next to histograms represent the corresponding GeoMFI. For NF-κB p65 **(E)** fold change was calculated by normalizing to the expression in unstimulated CD19$^+$ cells (set at value of 1). N = 3-4, P values were calculated using a mixed-effect analysis with Tukey's multiple comparison test, * $p < 0.05$, ** $p < 0.01$, **** $p < 0.0001$. Significance* is depicted if there is a significant difference between the green, red, purple or blue CD27/CD38 subpopulations.

 doi:10.20944/preprints202012.0028.v1

p-STAT5 analysis in the B cell subpopulations showed a gradual and transient increase in STAT5 phosphorylation over time, with prominent early induction of in the $CD27^{+}CD38^{+}$ ASC-population already after 6 hours of stimulation (Fig 3A). Interestingly, comparison of the four donors showed varying p-STAT5 profiles in the $CD27^{+}CD38^{+}$ ASC-populations, resulting in the high deviation of GeoMFI (Suppl. Fig. 4B). To further investigate this the $CD19^{+}$ p-STAT5 high population (FI > 1000) was gated on in two donors at multiple timepoints (Fig 3B-D). Even though these two donors showed a different profile of p-STAT5 within subpopulations at a GeoMFI level, the $p\text{-}STAT5^{high}$ cells found in both donors at several timepoints had similar CD27/CD38 expression profiles (Fig 3B-D, right). This demonstrates that these $p\text{-}STAT5^{high}$ cells are indeed induced in both donors at early timepoints in the $CD27^{+}CD38^{+}$ ASC-population, but that these can be overlooked when averaging values within subpopulations. Altogether, the data clearly shows that the simultaneous analysis of pSTAT5 and CD27 and CD38 differentiation markers in single cells allows for a more in-depth interrogation of B cell signaling across specific subpopulations, compared to using CD19 alone.

Preprints (www.preprints.org) | NOT PEER-REVIEWED | Posted: 2 December 2020 doi:10.20944/preprints202012.0028.v1

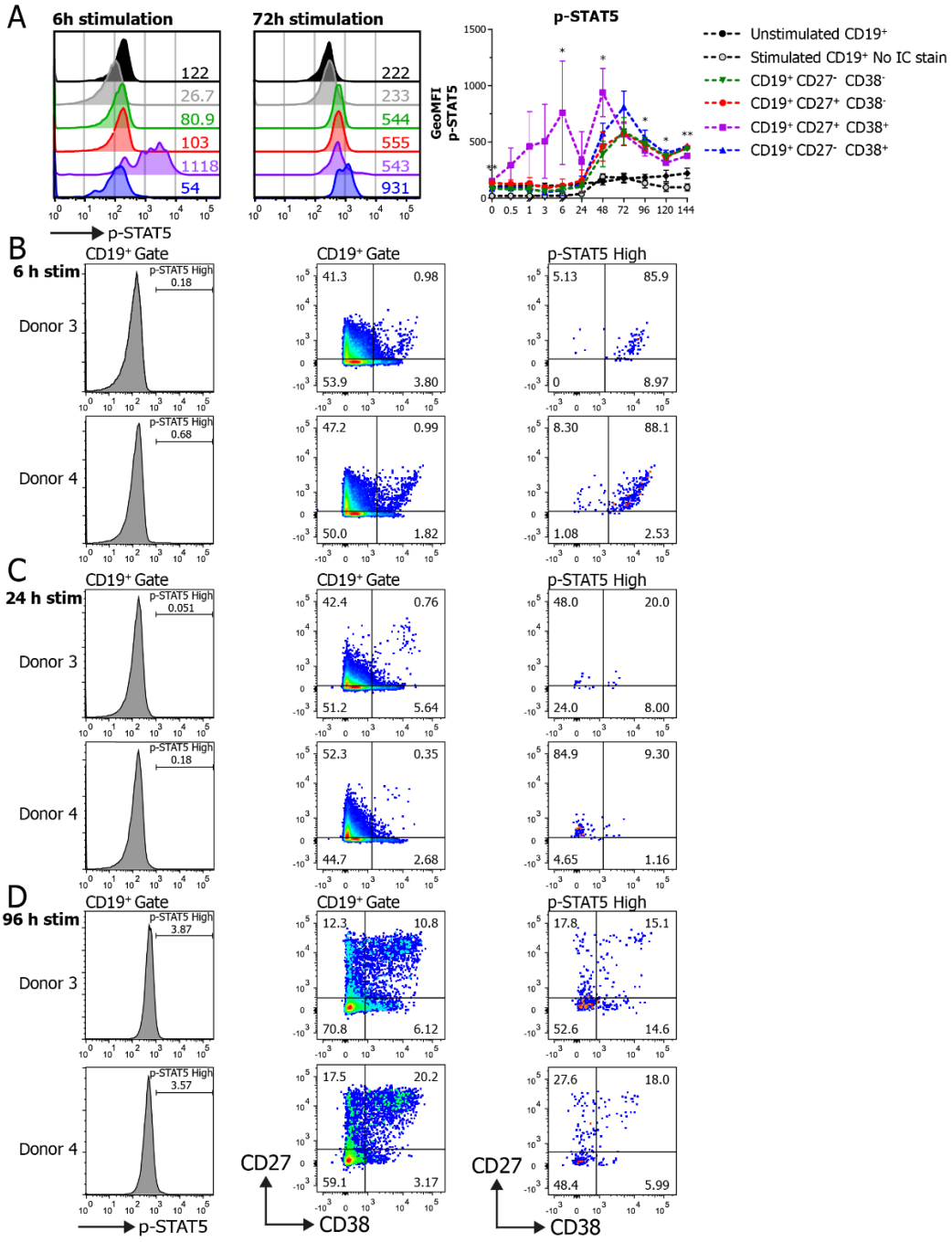

Figure 3. Phosphoflow analysis of STAT5 phosphorylation unveils heterogeneity over time in CD27/CD38 subpopulations. Human B cells (n=3-4) were stimulated with human-CD40L expressing 3T3 feeder layer, an anti-Ig F(ab)$_2$ mix (5 ug/ml) targeting IgM/IgG/IgA and recombinant cytokines IL-4 (25 ng/ml) and IL-21 (50 ng/ml) and multiple signaling proteins were analyzed by phosphoflow analysis over the course of 6-day culture. **(A)** Representative histogram overlays of p-STAT5 staining in CD19$^+$ and CD27/CD38 subpopulations after 6 h and 72 h stimulation (left) and the quantification of GeoMFI of p-STAT5 within the different subpopulations over the course of 6 days culture (right). Values depicted next to histograms represent the corresponding GeoMFI. N = 3-4, P values were calculated using a mixed-effect analysis with Tukey's multiple comparison test, * $p < 0.05$, ** $p < 0.01$, **** $p < 0.0001$. Significance is shown if there is a significant difference between the green, red, purple or blue CD27/CD38 subpopulations.**(B-D)** Histograms of p-STAT5 expression in the CD19$^+$ population in donor 3 and donor 4 (left) and the corresponding of CD27/CD38 expression profile in the CD19$^+$ population (middle) and p-STAT5 high expressing population (right) after 6 h **(B)**, 24 h **(C)** or 96 h **(D)** of stimulation.

 doi:10.20944/preprints202012.0028.v1

3.3 Sorted naïve and memory B cells show significant differences in response to varying CD40L, IL-21 and/or IL-4 stimuli

Next, naïve ($CD19^+$ $CD27^-$ IgD^+) and memory B cells ($CD19^+$ $CD27^+$) were sorted to further dissect intracellular signaling in naïve and memory B cells upon induction of B cell differentiation with various stimuli (Fig. 4A).

Clear p-STAT1 induction was observed through activation with CD40L in both naïve and memory B cells. The added presence of IL-21 further increase p-STAT1 levels in memory B cells (Fig. 4B). Although induction of p-STAT1 coincided with increased cell size, cell size alone did not fully account for p-STAT1 induction in memory B cells (Suppl. Fig. 5C-D).

Induction of p-STAT3 was the resultant of CD40L stimulation and amplified when IL-21 was also present in both naïve and memory B cells, irrespective of the presence of IL-4 (Fig. 4B-C).

Although BCR ligation yields p-STAT5 signaling, CD40L is the strongest inducer of p-STAT5 signaling, with naïve B cells being superior in p-STAT5 induction compared to memory B cells. (Fig. 4B-C).

In line with previous data[20]–[22]p-STAT6 is induced by IL-4, already after 30 minutes (Fig. 4C). This induction is amplified by CD40L. In addition, induction of p-STAT6 is significantly higher in naïve B cells compared to memory B cells. Activated NF-κB p65 was clearly induced when CD40L was present, already after 30 minutes of stimulation (Fig. 4B-C). In addition, activated NF-κB p65 was significantly higher in naïve B cells compared to memory B cells after 72 hours of stimulation. p-STAT3, 5 and 6 are induced by specific stimuli irrespective of cell size (Suppl. Fig. 5D). The higher induction of activated NF-κB p65 in naïve compared to memory B cells also indicates that this is induction that cannot fully be attributed to increased cell size.Altogether, these data show that the method presented here can be utilized to analyse the effects of crosstalk between BCR signaling and T_{FH}-derived CD40 and cytokine co-stimulation on STAT and NF-κB signaling in both naïve and memory B cells.

Preprints (www.preprints.org) | NOT PEER-REVIEWED | Posted: 2 December 2020 doi:10.20944/preprints202012.0028.v1

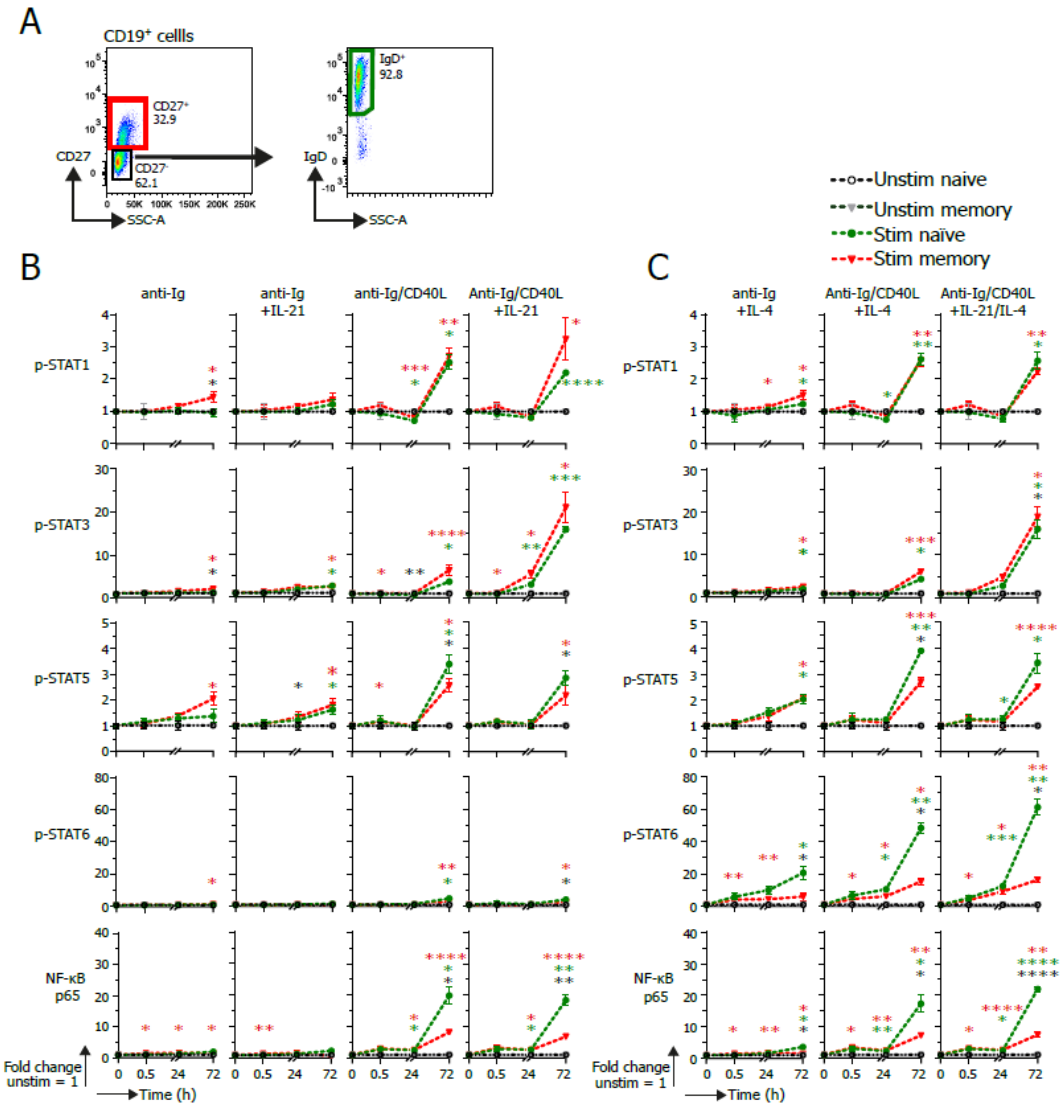

Figure 4. pSTAT and NF-κB signaling in naïve and memory B cells upon B cell activation via BCR, CD40 or IL4/Il-21. 10.000 human naïve ($CD19^+$ $CD27^-$ IgD^+) or memory ($CD19^+$ $CD27^+$) B cells (n=3) were stimulated after sorting with an anti-Ig $F(ab)_2$ mix (5 ug/ml) either or not together with a CD40L expressing 3T3 cells, recombinant cytokines IL-4 (25 ng/ml) and/or IL-21 (50 ng/ml). Multiple signaling proteins were analyzed by phosphoflow analysis up to 72h of stimulation. **(A)** Representative FACS plots of the sorting strategy for purification of $CD19^+$ $CD27^+$ memory and $CD19^+$ $CD27^-$ IgD^+ naïve B cells. **(B)** Quantification of GeoMFI of signaling proteins in stimulated sorted naïve or memory B cells after 30min, 24h or 72h stimulation with varying IL-21 stimulations. Fold change was calculated normalizing expression to unstimulated condition. P values were calculated using a mixed-effect analysis with Tukey's multiple comparison test. * $p < 0.05$, ** $p < 0.01$, **** $p < 0.0001$. Red* shows significance of stimulated memory compared to unstimulated, green* shows significance of stimulated naïve compared to unstimulated and black* shows significance of stimulated naïve vs stimulated memory. **(C)** Quantification of GeoMFI of signaling proteins in stimulated sorted naïve or memory B cells after 30min, 24h or 72h stimulation with varying IL-4 stimulations. Fold change was calculated normalizing the expression to the respective unstimulated condition. P values were calculated by using a mixed-effect analysis with Tukey's multiple comparison test. * $p < 0.05$, ** $p < 0.01$, **** $p < 0.0001$. Red* shows significance of stimulated memory compared to unstimulated, green* shows significance of stimulated naïve compared to unstimulated and black* shows significance of stimulated naïve vs stimulated memory

 doi:10.20944/preprints202012.0028.v1

3.4. TF – flow assay allows for a high-resolution analysis of TFs within subpopulations

Next, a flow cytometric assay to detect known B cell transcription factors (Fig. 5A) within B cell subpopulations was set up. To validate TF – flow analyses, the TF protein expression levels measured by flow were compared to mRNA expression levels measured by semiquantitative PCR. First, after a 6-day stimulation the B cell subpopulations were sorted based on CD27 and CD38 expression (Fig. 5B). Subsequently, mRNA expression of the transcription factors PAX5, c-MYC, BCL6, BLIMP1, XBP-1 and AICDA were measured by semiquantitative PCR (Fig. 5C). As expected, mRNA expression of PAX5, c-MYC and AICDA was significantly downregulated in the CD27+CD38+ population compared to other populations. Additionally, expression of BLIMP1 and XBP-1 was increased. Altogether indicating that the CD27+CD38+ B cells have transitioned from a B cell mRNA expression profile to an ASC mRNA expression profile as the B cell signature gene PAX5 is downregulated and ASC-related genes BLIMP1 and XBP-1 are upregulated (Fig. 5A). Next, the same experiment was performed but now the transcription factors were stained within the different B cell subpopulations (Fig. 5C-D). As the reagents in the Foxp3 staining kit greatly reduce cell size (making it impossible to gate on a lymphocyte population) cells were first gated on live cells before doublet exclusion and gating for CD19 and CD27/CD38 subpopulations. The protein expression profiles of all transcription factors within subpopulations are highly comparable to the mRNA data. The expression of TFs was not dependent on cell size (Suppl. Fig. 6B). Furthermore, there is a clear downregulation of CD19 in the $CD27^{+}CD38^{+}$ ASC population that coincides with a downregulation of PAX5 and an upregulation of BLIMP1 (Suppl. Fig. 6C). The clear advantage of these TF analyses by flow cytometry is that it allows for detection of protein instead of mRNA. Another advantage is the added depth of analyses, as demonstrated by the observed bimodal expression of PAX5 and BLIMP1 within the $CD27^{+}CD38^{-}$ and $CD27^{-}CD38^{+}$ populations (Fig. 5E, right), that could not be detected in the mRNA expression analysis.

Preprints (www.preprints.org) | NOT PEER-REVIEWED | Posted: 2 December 2020 doi:10.20944/preprints202012.0028.v1

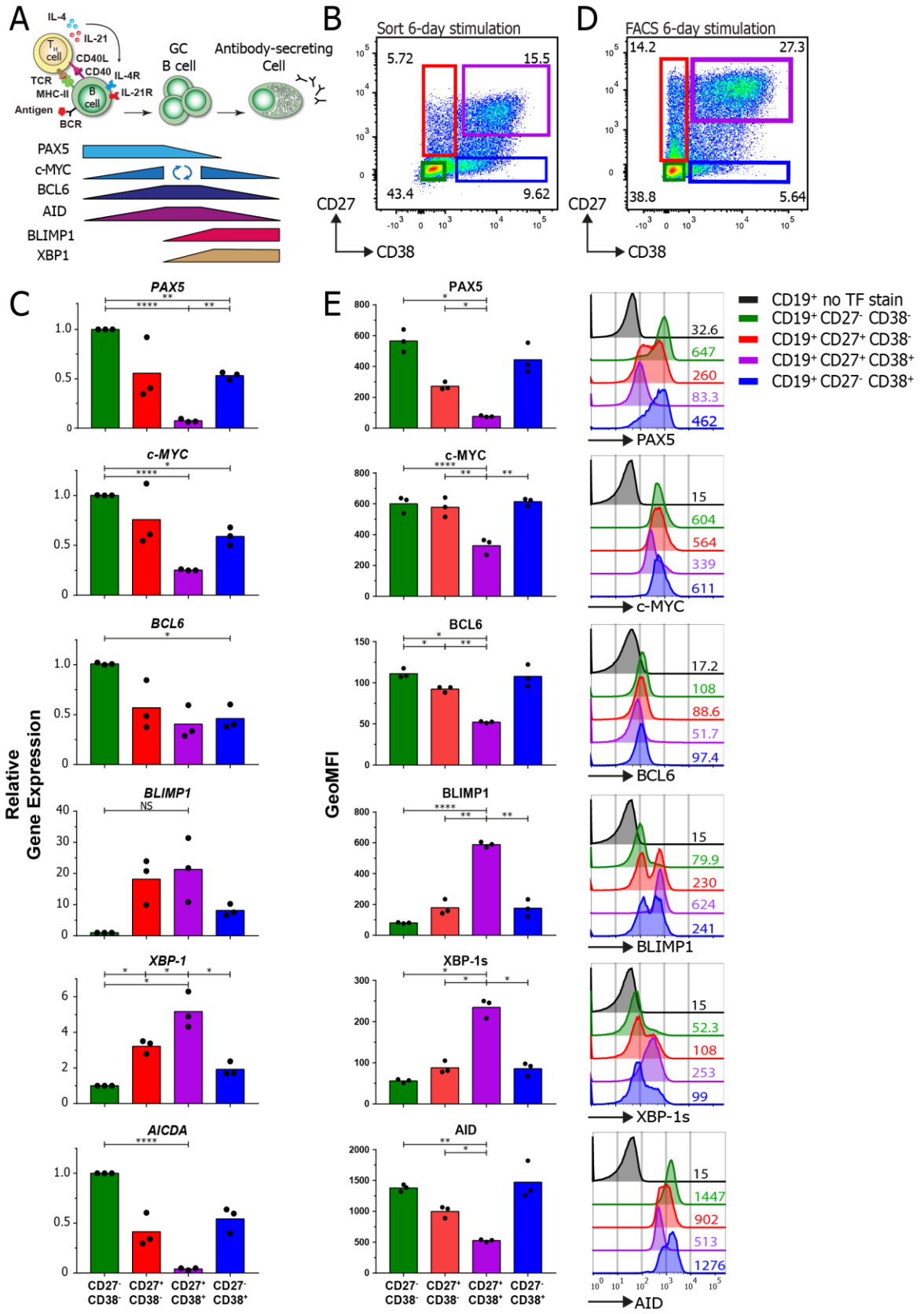

Figure 5. Transcription factor analysis in stimulated human B cells by flow cytometry. Human B cells (n=3) were stimulated with an anti-Ig F(ab)2 mix (5 ug/ml) and recombinant cytokines IL-4 (25 ng/ml) and IL-21 (50 ng/ml) for 6 days and analyzed for the mRNA and protein expression of multiple transcription factors. **(A)** Schematic representation of the expression of B cell-, GC cell- and ASC-defining transcription factors after T cell-dependent B cell stimulation. **(B)** Representative FACS plot

 doi:10.20944/preprints202012.0028.v1

of the sorting strategy of the CD27/CD38 subpopulations for analysis by semiquantitative RT-PCR. A more stringent gating strategy was used here to prevent contamination of subpopulations during sorting. **(C)** Quantification of relative gene expression of *PAX5*, *c-MYC, BCL6*, *BLIMP1*, *XBP-1* and *AICDA* in different CD27/CD38 subpopulations as measured by semiquantitative RT-PCR. All results were normalized to the internal control 18S rRNA. Expression is calculated relatively to the $CD27^-CD38^-$ subpopulation (set at value of 1). Each dot represents an independent donor and mean values are represented as bars (n=3). **(D)** Representative FACS plot of the CD27/CD38 subpopulations that were stained for transcription factors and analyzed by FACS. **(E)** Quantification of the GeoMFI of PAX5, c-MYC, BCL6, BLIMP1, XBP-1s (active spliced isoform) and AID stained for in different CD27/CD38 subpopulations (left) and corresponding histogram overlays (right). Values depicted next to histograms represent the corresponding GeoMFI. Each dot represents an independent donor and mean values are represented as bars (n=3). P values were calculated using Tukey's multiple comparison test, * $p < 0.05$, ** $p < 0.01$, **** $p < 0.0001$.

3.5. UMAP analysis unravels B cell subpopulation heterogeneity

To further investigate the heterogenous expression of transcription factors within B cell subpopulations on a single-cell level, a UMAP analysis was performed on the flow cytometric data (Fig. 6). Cells from either $CD27^-CD38^-$ population or the $CD27^+CD38^+$ population cluster together, as seen in the UMAP overlay of B cell subpopulations (Fig. 6A) and the heatmap expression plots (Fig. 6B). Neither the $CD27^+CD38^-$ population or the $CD27^-CD38^+$ population form a uniform cluster. Notably and in line with the mutual exclusive expression patterns of PAX5 (denoting B cell signature) and BLIMP1 (denoting ASC signature), the heatmaps of PAX5 and BLIMP1 clearly show a mirrored pattern, where PAX5 expression is down BLIMP1 expression is increased. Strikingly, the UMAP analyses bring to light a small cluster of BCL6 high expressing cells located on the border of the $CD27^+CD38^+$ cluster (Fig. 6B, lower-right). As this population is not noted when plotting only the GeoMFI of CD27/CD38 subsets, these data show the clear added benefit of applying UMAP analyses on data generated with this TF flow method. As expression of PAX5 and BLIMP1 was bimodal in the $CD27^+CD38^-$ and $CD27^-CD38$ populations (Fig. 5E), this heterogeneity was further elucidated by comparing the heatmap expression of CD27, PAX5 and BLIMP1 (Fig. 6C). The data show that the expression of CD27 coincides with BLIMP1 expression (and therefore negatively coincides with PAX5 expression). Similar patterns are seen for CD38 in the $CD27^-CD38^+$ population. Together, these heatmaps explain the bimodal expressions seen in Fig. 4E. Altogether this data shows that the TF – flow protocol can be used to efficiently stain TFs within B cell subpopulations. This technique allows for a relatively fast analysis of TF-expression at a single-cell resolution, a major advantage over mRNA-expression analysis where populations have to be sorted. In addition, this method and UMAP analysis allow for uncovering of small populations that have unique TF expression profiles.

Preprints (www.preprints.org) | NOT PEER-REVIEWED | Posted: 2 December 2020 doi:10.20944/preprints202012.0028.v1

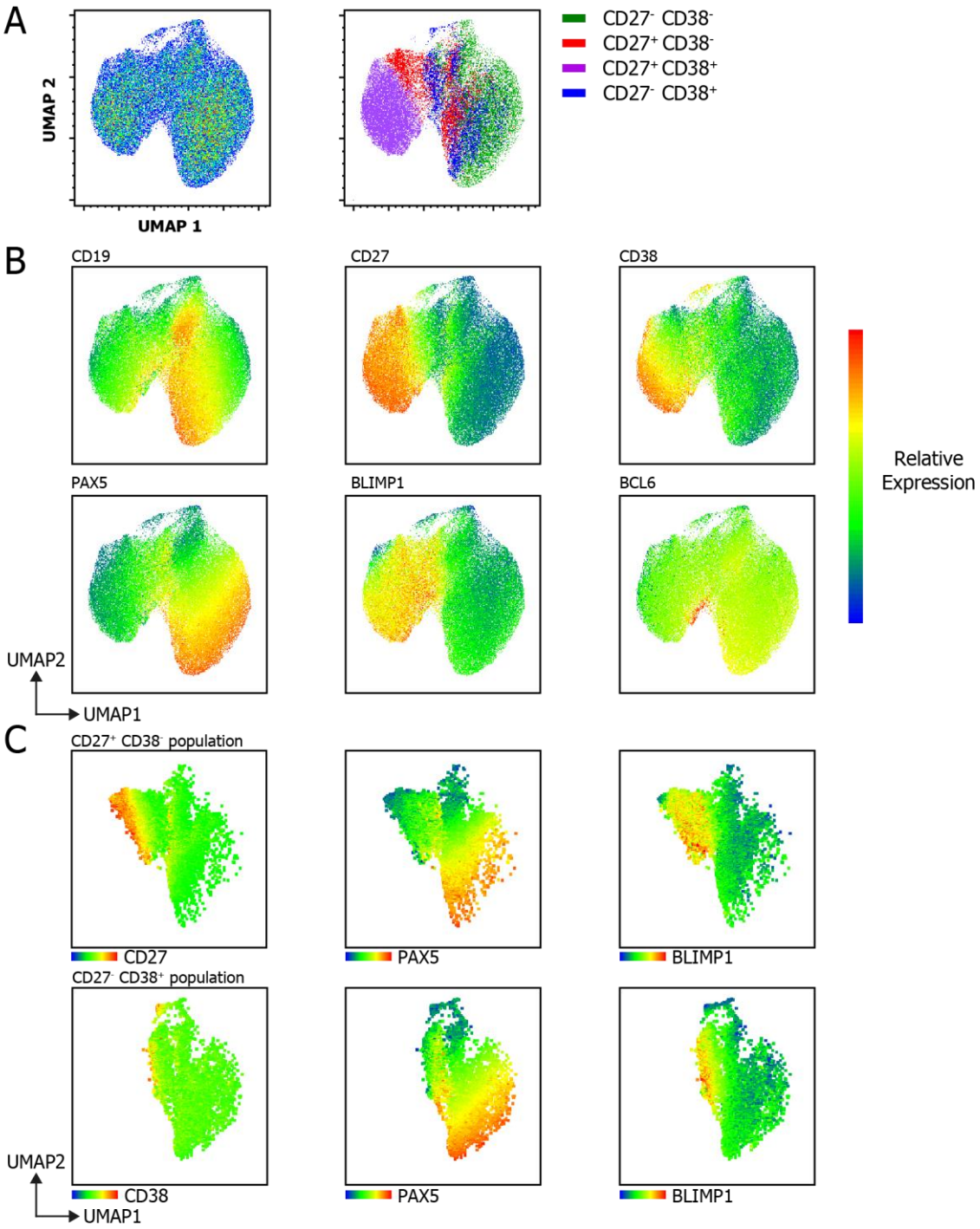

Figure 6. UMAP analysis of combined membrane marker and TF marker analyses upon B cell differentiation. UMAP clustering analysis on B cells stained for CD19, CD27, CD38, PAX5, BLIMP1 and BCL6 after 6-day culture with a human-CD40L expressing 3T3 feeder layer, an anti-Ig F(ab)$_2$ mix (5 ug/ml) targeting IgM/IgG/IgA and recombinant cytokines IL-4 (25 ng/ml) and IL-21 (50 ng/ml). **(A)** UMAP 2D scatter plot of 60,000 living single CD19$^+$ B cells from 3 donors (left) and the different CD27/CD38 subpopulations overlaid (right). UMAP settings were as followed: Distance function Euclidean; number of neighbours 30; minimal distance 0.5 and number of components 2. **(B)** Heatmap of the relative protein expression of CD19, CD27, CD38, PAX5, BLIMP1 and BCL6 included in the UMAP analysis overlaid on the UMAP 2D scatter plot. **(C)** Heatmap of the relative protein expression of PAX5 and BLIMP1 within the isolated CD27$^+$CD38$^-$ population (top) and CD27$^-$CD38$^+$ population (bottom) overlaid on the UMAP 2D scatter plot.

 doi:10.20944/preprints202012.0028.v1

4. Discussion

Here we present a protocol for the detection and monitoring of signaling via phosphorylated STAT and activated NF-κB p65 within several B cell subpopulations. Furthermore, a second method is presented here that allows for detection of TFs within B cell subpopulations. Both flow cytometric-based methods provide a clear advantage over other techniques like western blotting or detection of mRNA. First, cells do not have to be purified prior to analysis and MM can be used to distinguish differentiated B cell subpopulations. Furthermore, these methods allow for analysis at a single-cell level for more in-depth analyses of cell signaling and TF expression in specific cellular subpopulations. In addition, these methods are optimized for sample processing in a 96-well format, allowing for a high throughput analysis. Finally, one major advantage of this methanol-based phosphoflow method is that samples can be stored in the freezer for prolonged periods of time [51]. This allowed for the harvesting of multiple timepoints over the course of a 6-day culture and staining intracellular phospho-proteins of multiple samples simultaneously. One drawback of these methods is the lack of commercially available conjugated antibodies with a wide range of fluorophores. Not all fluorophores or antibodies maintain reactivity under the phosphoflow protocol as also noted by others [45, 51, 52]. Additionally, antibodies directed against nuclear TFs are currently only available in a small selection of fluorophores. This makes it difficult to combine several TF-targeting antibodies into a single panel. When setting up the transcription flow within one's own lab it is advised to reserve the brightest fluorophores, like PE-Cy7 and AF647, for antibodies targeting the nuclear TFs. This ensures the highest resolution of detection of these, sometimes lowly expressed, TFs. Fortunately, the availability of antibodies and fluorophores is constantly expanding and this will most likely allow for a more extensive panel in the near future.

Using these phosphoflow and TF – flow methods several observations were made. First, B cell subsets showed significantly different steady state levels of phosphorylated STAT1 and STAT6. Mainly the $CD27^{+}CD38^{-}$ subset, conventionally called memory B cells, and the $CD27^{+}CD38^{+}$ ASC-population had significantly higher levels of phosphorylated STAT1 and STAT6. Furthermore, all the measured intracellular signaling proteins are more rapidly induced and also decline earlier in these subsets compared to the $CD27^{-}CD38^{-}$ and $CD27^{-}CD38^{+}$ populations. Interestingly, when naïve and memory B cells are compared, p-STAT6 induction is much higher in naïve B cells compared to memory B cell. In both subsets, p-STAT6 is induced by IL-4 as shown previously [20]–[22] and this induction is amplified if CD40L is present. In addition, p-STAT5 and activated NF-κB p65 levels are significantly higher in naïve B cells compared to memory B cells under specific stimuli. These data confirm previous findings that NF-kB p65 induction is higher in naïve compared to memory B cells[52]. Furthermore, in a different *in vitro* stimulation system it was shown that p-STAT 5 was more rapidly induced in naïve B cells compared to memory B cells [53]. However, in that paper IL-21 was used as a stimulus. The data presented here show that IL-4 in fact induces and maintains higher levels of p-STAT5 compared to IL-21 as there was no dip in p-STAT5 at the 24-hour timepoint when IL-4 was present. Furthermore, it was previously shown that p-STAT1 and p-STAT3 induction is higher in naïve B cells and is induced mainly by IL-21[23], [53]. This contradicts the data presented here where p-STAT1 and p-STAT3 levels are higher in memory B cells compared to naïve B cells after stimulation. In addition, p-STAT1 is already induced by CD40L alone and further increased by IL-21 in memory B cells. Similarly, the data presented here shows that CD40L already induces p-STAT3 in both memory and naïve B cells and that this induction is amplified by IL-21. The main differences between the previously mentioned *in vitro* system[53] and the one utilized here is that the authors had to sort the splenic B cell subsets instead of circulating B cells and that these cells were pre-stimulated with anti-Ig/CD40L before adding cytokines and measuring phosphorylation of signaling proteins. Another observation is the rapid induction of p-STAT5 in the $CD27^{+}CD38^{+}$ ASC-population in the first hours of stimulation. As these p-STAT5 high $CD27^{+}CD38^{+}$ cells are almost all gone after 24 hours, it is likely that this induction is specific to *ex vivo* circulating plasmablasts present in the culture. These cells are however not sustained within this system. To the best of our knowledge this induction has not been shown before. The regulation of p-STAT5 in B cells remains largely unknown. It has been shown that p-STAT5 can induce but also inhibit BCL6 expression [54–56]. As BCL6 is

tightly linked to survival and proliferation of B cells [57], this induction of p-STAT5 in the $CD27^{+}CD38^{+}$ ASC-population could be linked to the survival of these cells after *in vitro* stimulation. Additionally, cells with high levels of p-STAT5 found throughout the culture may have a different capacity to survive and proliferate compared to the other cells. Combining the phosphoflow method here with cell trace proliferation dyes could help further elucidate this. To ensure that differences in signaling profiles in stimulated B cell subsets were not due differences in cell size, the FSC-A parameter was investigated as an indication of size. It was shown that indeed after prolonged culture and stimulation, the FSC-A increased. However, this increase does not correlate with the increases in p-STAT and NF-κB levels, showing that the induction was specific to the stimuli provided. As the increased cell size could lead to increased total-STAT levels these should be investigated and compared to p-STAT induction. This was not done here as the flow panel did not allow the addition of antibodies directed against all total-STAT proteins.

The TF – flow method revealed a previously unappreciated heterogeneity of PAX5 and BLIMP1 expression in the $CD27^{+}CD38^{-}$ and $CD27^{-}CD38^{+}$. Furthermore, a high BCL6 expressing population was found that could not have been detected by measuring mRNA in bulk sorted populations. As high expression of BCL6 is a hallmark of GC B cells, this BCL6-high population could be *in vitro* induced GC B cells. Together this data shows that the single-cell resolution gained with this flow cytometric method will allow for further in-depth identification of distinct B cell subsets and elucidation of specific intracellular signaling and TF expression over time.

The methods presented here allow for a sensitive and efficient analysis of signaling proteins and TFs, together with MM. These methods allow for analysis at a single-cell resolution that can aid immunomonitoring of signaling and transcriptional regulation in healthy, and harmful B cell responses, like RA, lupus, vasculitis and allo-antibody formation [38–41]. Additionally, these techniques can aid in the development and characterization of therapeutic inhibitors [44]. Furthermore, as different B cell subsets have been known and shown here to have varying and dynamic regulation of signaling [53, 58], the methods presented here will help fundamental research further investigate this.

Supplementary Materials:

Figure S1: Preservation of antibody reactivity against MM for B cell differentiation upon fixation and permeabilization of PBMCs, Figure S2: Representative gating strategy for the gating of $CD19^{+}$ B cells, Figure S3: Representative histograms of phosphoflow analysis at different time points of B cell differentiation., Figure S4: NF-κBNF-κB p65 and p-STAT5 expression of 4 individual donors, Figure S5. Relationship between pSTAT/NF-κB p65 signals and cell size during B cell differentiation., Figure S6. Stimulated CD27/CD38 subpopulations show significant differences in CD19 expression and FSC-A during TF-flow analysis**Author Contributions:** C.M designed and performed all laboratory experiments, data analyses and generated all figures. T.J performed and analyzed all of the semiquantitative-PCR. A.t.B contributed to supervision. S.M.v.H main supervisor. All authors contributed to writing of the manuscript. All authors have read and agreed to the published version of the manuscript

Funding: This project was funded by the Landsteiner Foundation for Blood Transfusion Research, project grant number: LSBR 1609 and Sanquin Product and Process Development Call 2020.

Acknowledgments: We thank Simon Tol, Erik Mul, Mark Hoogenboezem and Tom Ebbes of the Sanquin central facility for cell sorting on the FACS AriaIII and maintenance and calibration of FACS machines.

Conflicts of Interest: The authors declare no conflict of interest. The funders had no role in the design of the study; in the collection, analyses, or interpretation of data; in the writing of the manuscript, or in the decision to publish the results.

References

[1] C. King, S. G. Tangye, and C. R. Mackay, " T Follicular Helper (T FH) Cells in Normal and Dysregulated Immune Responses ," *Annu. Rev. Immunol.*, vol. 26, no. 1, pp. 741–766, Apr. 2008, doi: 10.1146/annurev.immunol.26.021607.090344.

[2] R. L. Reinhardt, H. E. Liang, and R. M. Locksley, "Cytokine-secreting follicular T cells shape the antibody

repertoire," *Nat. Immunol.*, vol. 10, no. 4, pp. 385–393, 2009, doi: 10.1038/ni.1715.

[3] Z. Shulman *et al.*, "Dynamic signaling by T follicular helper cells during germinal center B cell selection," *Science (80-.).*, vol. 345, no. 6200, pp. 1058–1062, Aug. 2014, doi: 10.1126/science.1257861.

[4] K. Rajewsky, "Clonal selection and learning in the antibody system," *Nature*, vol. 381, no. 6585. pp. 751–758, Jun. 27, 1996, doi: 10.1038/381751a0.

[5] A. D. Gitlin, Z. Shulman, and M. C. Nussenzweig, "Clonal selection in the germinal centre by regulated proliferation and hypermutation.," *Nature*, vol. 509, no. 7502, pp. 637–40, 2014, doi: 10.1038/nature13300.

[6] L. J. McHeyzer-Williams, N. Pelletier, L. Mark, N. Fazilleau, and M. G. McHeyzer-Williams, "Follicular helper T cells as cognate regulators of B cell immunity," *Current Opinion in Immunology*, vol. 21, no. 3. Elsevier Current Trends, pp. 266–273, Jun. 01, 2009, doi: 10.1016/j.coi.2009.05.010.

[7] Y. Takahashi, P. R. Dutta, D. M. Cerasoli, and G. Kelsoe, "In situ studies of the primary immune response to (4-hydroxy-3- nitrophenyl)acetyl. v. affinity maturation develops in two stages of clonal selection," *J. Exp. Med.*, vol. 187, no. 6, pp. 885–895, Mar. 1998, doi: 10.1084/jem.187.6.885.

[8] F. J. Weisel, G. V. Zuccarino-Catania, M. Chikina, and M. J. Shlomchik, "A Temporal Switch in the Germinal Center Determines Differential Output of Memory B and Plasma Cells," *Immunity*, vol. 44, no. 1, pp. 116–130, 2016, doi: 10.1016/j.immuni.2015.12.004.

[9] D. Zotos *et al.*, "IL-21 regulates germinal center B cell differentiation and proliferation through a B cell-intrinsic mechanism.," *J. Exp. Med.*, vol. 207, no. 2, pp. 365–78, Feb. 2010, doi: 10.1084/jem.20091777.

[10] B. B. Ding, E. Bi, H. Chen, J. J. Yu, and B. H. Ye, "IL-21 and CD40L Synergistically Promote Plasma Cell Differentiation through Upregulation of Blimp-1 in Human B Cells," *J. Immunol.*, vol. 190, no. 4, pp. 1827–1836, Feb. 2013, doi: 10.4049/jimmunol.1201678.

[11] L. Moens and S. G. Tangye, "Cytokine-mediated regulation of plasma cell generation: IL-21 takes center stage," *Frontiers in Immunology*, vol. 5, no. FEB. Frontiers Research Foundation, p. 65, Feb. 18, 2014, doi: 10.3389/fimmu.2014.00065.

[12] I. Yusuf *et al.*, "Germinal Center T Follicular Helper Cell IL-4 Production Is Dependent on Signaling Lymphocytic Activation Molecule Receptor (CD150)," *J. Immunol.*, vol. 185, no. 1, pp. 190–202, Jul. 2010, doi: 10.4049/jimmunol.0903505.

[13] J. S. Weinstein *et al.*, "TFH cells progressively differentiate to regulate the germinal center response," *Nat. Immunol.*, vol. 17, no. 10, pp. 1197–1205, 2016, doi: 10.1038/ni.3554.

[14] H. Gascan, J. F. Gauchat, M. G. Roncarolo, H. Yssel, H. Spits, and J. E. De Vries, "Human B cell clones can be induced to proliferate and to switch to IgE and IgG4 synthesis by interleukin 4 and a signal provided by activated CD4+ T cell clones," *J. Exp. Med.*, vol. 173, no. 3, pp. 747–750, 1991, doi: 10.1084/jem.173.3.747.

[15] D. T. Avery, V. L. Bryant, C. S. Ma, R. de Waal Malefyt, and S. G. Tangye, "IL-21-Induced Isotype Switching to IgG and IgA by Human Naive B Cells Is Differentially Regulated by IL-4," *J. Immunol.*, vol. 181, no. 3, pp. 1767–1779, Aug. 2008, doi: 10.4049/jimmunol.181.3.1767.

[16] D. G. Gonzalez *et al.*, "Nonredundant Roles of IL-21 and IL-4 in the Phased Initiation of Germinal Center B Cells and Subsequent Self-Renewal Transitions," *J. Immunol.*, p. ji1500497, 2018, doi: 10.4049/jimmunol.1500497.

[17] A. Craxton, G. Shu, J. D. Graves, J. Saklatvala, E. G. Krebs, and E. A. Clark, "p38 MAPK is required for CD40-induced gene expression and proliferation in B lymphocytes.," *J. Immunol.*, vol. 161, no. 7, pp. 3225–36, Oct. 1998, Accessed: May 10, 2020. [Online]. Available: http://www.ncbi.nlm.nih.gov/pubmed/9759836.

[18] D. Chen *et al.*, "CD40-Mediated NF-κB Activation in B Cells Is Increased in Multiple Sclerosis and Modulated by Therapeutics," *J. Immunol.*, vol. 197, no. 11, pp. 4257–4265, Dec. 2016, doi: 10.4049/jimmunol.1600782.

[19] S. C. Sun, "The non-canonical NF-κB pathway in immunity and inflammation," *Nature Reviews Immunology*, vol. 17, no. 9. Nature Publishing Group, pp. 545–558, Sep. 01, 2017, doi: 10.1038/nri.2017.52.

[20] M. B. Harris *et al.*, "Transcriptional Repression of Stat6-Dependent Interleukin-4-Induced Genes by BCL-6: Specific Regulation of Iε Transcription and Immunoglobulin E Switching," *Mol. Cell. Biol.*, vol. 19, no. 10, pp. 7264–7275, Oct. 1999, doi: 10.1128/mcb.19.10.7264.

[21] A. L. Wurster, V. L. Rodgers, M. F. White, T. L. Rothstein, and M. J. Grusby, "Interleukin-4-mediated protection of primary B cells from apoptosis through Stat6-dependent up-regulation of Bcl-xL," *J. Biol. Chem.*, vol. 277, no. 30, pp. 27169–27175, 2002, doi: 10.1074/jbc.M201207200.

[22] D. T. Avery *et al.*, "STAT3 is required for IL-21 induced secretion of IgE from human naive B cells," *Blood*, vol. 112, no. 5, pp. 1784–1793, Sep. 2008, doi: 10.1182/blood-2008-02-142745.

[23] D. T. Avery *et al.*, "B cell-intrinsic signaling through IL-21 receptor and STAT3 is required for establishing long-lived antibody responses in humans," *J. Exp. Med.*, vol. 207, no. 1, pp. 155–171, 2010, doi: 10.1084/jem.20091706.

[24] J. E. Darnell, I. M. Kerr, and G. R. Stark, "Jak-STAT pathways and transcriptional activation in response to IFNs and other extracellular signaling proteins," *Science (80-.).*, vol. 264, no. 5164, pp. 1415–1421, 1994, doi: 10.1126/science.8197455.

[25] A. Oeckinghaus and S. Ghosh, "The NF-kappaB family of transcription factors and its regulation.," *Cold Spring Harbor perspectives in biology*, vol. 1, no. 4. Cold Spring Harbor Laboratory Press, 2009, doi: 10.1101/cshperspect.a000034.

[26] P. Tuijnenburg *et al.*, "Loss-of-function nuclear factor κB subunit 1 (NFKB1) variants are the most common monogenic cause of common variable immunodeficiency in Europeans," *J. Allergy Clin. Immunol.*, vol. 142, no. 4, pp. 1285–1296, Oct. 2018, doi: 10.1016/j.jaci.2018.01.039.

[27] G. D. Victora and M. C. Nussenzweig, "Germinal Centers," doi: 10.1146/annurev-immunol-020711-075032.

[28] L. Mesin, J. Ersching, and G. D. Victora, "Germinal Center B Cell Dynamics," *Immunity*, vol. 45, no. 3, pp. 471–482, 2016, doi: 10.1016/j.immuni.2016.09.001.

[29] N. S. De Silva and U. Klein, "Dynamics of B cells in germinal centres," *Nat. Rev. Immunol.*, vol. 15, no. 3, pp. 137–148, 2015, doi: 10.1038/nri3804.

[30] C. Cobaleda, A. Schebesta, A. Delogu, and M. Busslinger, "Pax5: The guardian of B cell identity and function," *Nature Immunology*, vol. 8, no. 5. pp. 463–470, May 2007, doi: 10.1038/ni1454.

[31] H. L. Chang *et al.*, "Regulation of the germinal center gene program by interferon (IFN) regulatory factor 8/IFN consensus sequence-binding protein," *J. Exp. Med.*, vol. 203, no. 1, pp. 63–72, Jan. 2006, doi: 10.1084/jem.20051450.

[32] D. Pedro Calado *et al.*, "MYC is essential for the formation and maintenance of germinal centers HHS Public Access," *Nat Immunol*, vol. 13, no. 11, pp. 1092–1100, 2012, doi: 10.1038/ni.2418.

[33] S. L. Nutt, P. D. Hodgkin, D. M. Tarlinton, and L. M. Corcoran, "The generation of antibody-secreting plasma cells," *Nat. Rev. Immunol.*, vol. 15, no. 3, pp. 160–171, Mar. 2015, doi: 10.1038/nri3795.

[34] S. Finkin, H. Hartweger, T. Y. Oliveira, E. E. Kara, and M. C. Nussenzweig, "Protein Amounts of the MYC Transcription Factor Determine Germinal Center B Cell Division Capacity," *Immunity*, vol. 51, no. 2, pp. 324-336.e5, 2019, doi: 10.1016/j.immuni.2019.06.013.

[35] S. L. Nutt, P. D. Hodgkin, D. M. Tarlinton, and L. M. Corcoran, "The generation of antibody-secreting plasma cells.," *Nat. Rev. Immunol.*, vol. 15, no. 3, pp. 160–171, 2015, doi: 10.1038/nri3795.

[36] J. Tellier and S. L. Nutt, "Plasma cells: The programming of an antibody-secreting machine," *Eur. J. Immunol.*, vol. 49, no. 1, pp. 30–37, Jan. 2019, doi: 10.1002/eji.201847517.

[37] H. Yoshida, T. Matsui, A. Yamamoto, T. Okada, and K. Mori, "XBP1 mRNA is induced by ATF6 and spliced by IRE1 in response to ER stress to produce a highly active transcription factor," *Cell*, vol. 107, no. 7, pp. 881–891, Dec. 2001, doi: 10.1016/S0092-8674(01)00611-0.

[38] S. Bugatti, B. Vitolo, R. Caporali, C. Montecucco, and A. Manzo, "B cells in rheumatoid arthritis: From pathogenic players to disease biomarkers," *Biomed Res. Int.*, vol. 2014, 2014, doi: 10.1155/2014/681678.

[39] D. Y. H. Yap and T. M. Chan, "B cell abnormalities in systemic lupus erythematosus and lupus nephritis—role in pathogenesis and effect of immunosuppressive treatments," *International Journal of Molecular Sciences*, vol. 20, no. 24. MDPI AG, Dec. 02, 2019, doi: 10.3390/ijms20246231.

[40] M. McClure, S. Gopaluni, D. Jayne, and R. Jones, "B cell therapy in ANCA-associated vasculitis: current and emerging treatment options," *Nature Reviews Rheumatology*, vol. 14, no. 10. Nature Publishing Group, pp. 580–591, Oct. 01, 2018, doi: 10.1038/s41584-018-0065-x.

[41] K. Pavenski, J. Freedman, and J. W. Semple, "HLA alloimmunization against platelet transfusions: pathophysiology, significance, prevention and management," *Tissue Antigens*, vol. 79, no. 4, pp. 237–245, Apr. 2012, doi: 10.1111/j.1399-0039.2012.01852.x.

[42] O. de Barrios, A. Meler, and M. Parra, "MYC's Fine Line Between B Cell Development and Malignancy," *Cells*, vol. 9, no. 2, p. 523, Feb. 2020, doi: 10.3390/cells9020523.

[43] A. L. Shaffer, R. M. Young, and L. M. Staudt, "Pathogenesis of Human B Cell Lymphomas," *Annu. Rev. Immunol.*, vol. 30, no. 1, pp. 565–610, Apr. 2012, doi: 10.1146/annurev-immunol-020711-075027.

[44] Y. Jamilloux, T. El Jammal, L. Vuitton, M. Gerfaud-Valentin, S. Kerever, and P. Sève, "JAK inhibitors for the treatment of autoimmune and inflammatory diseases," *Autoimmunity Reviews*, vol. 18, no. 11. Elsevier B.V., Nov. 01, 2019, doi: 10.1016/j.autrev.2019.102390.

[45] J. Rip, M. J. W. de Bruijn, A. Kaptein, R. W. Hendriks, and O. B. J. Corneth, "Phosphoflow Protocol for Signaling Studies in Human and Murine B Cell Subpopulations," *J. Immunol.*, p. ji1901117, 2020, doi: 10.4049/jimmunol.1901117.

[46] P. O. Krutzik, M. R. Clutter, and G. P. Nolan, "Coordinate Analysis of Murine Immune Cell Surface Markers and Intracellular Phosphoproteins by Flow Cytometry 1," 2005.

[47] M. Urashima, D. Chauhan, H. Uchiyama, G. J. Freeman, and K. C. Anderson, "CD40 ligand triggered interleukin-6 secretion in multiple myeloma," *Blood*, vol. 85, no. 7, pp. 1903–1912, 1995, doi: 10.1182/blood.v85.7.1903.bloodjournal8571903.

[48] T. Karonitsch *et al.*, "Activation of the interferon-gamma signaling pathway in systemic lupus erythematosus peripheral blood mononuclear cells.," *Arthritis Rheum.*, vol. 60, no. 5, pp. 1463–71, 2009, doi: 10.1002/art.24449.

[49] N. Schmitt *et al.*, "The cytokine TGF-β 2 co-opts signaling via STAT3-STAT4 to promote the differentiation of human T FH cells," *Nat. Immunol.*, vol. 15, no. 9, pp. 856–865, 2014, doi: 10.1038/ni.2947.

[50] Y. Souwer *et al.*, "Detection of aberrant transcription of major histocompatibility complex class II antigen presentation genes in chronic lymphocytic leukaemia identifies *HLA-DOA* mRNA as a prognostic factor for survival," *Br. J. Haematol.*, vol. 145, no. 3, pp. 334–343, May 2009, doi: 10.1111/j.1365-2141.2009.07625.x.

[51] P. O. Krutzik and G. P. Nolan, "Intracellular phospho-protein staining techniques for flow cytometry:

Monitoring single cell signaling events," *Cytometry*, vol. 55A, no. 2, pp. 61–70, Oct. 2003, doi: 10.1002/cyto.a.10072.

[52] K. Huse *et al.*, "Human Germinal Center B Cells Differ from Naïve and Memory B Cells in CD40 Expression and CD40L-Induced Signaling Response," *Cytom. Part A*, vol. 95, no. 4, pp. 442–449, Apr. 2019, doi: 10.1002/cyto.a.23737.

[53] E. K. Deenick *et al.*, "Naive and memory human B cells have distinct requirements for STAT3 activation to differentiate into antibody-secreting plasma cells.," *J. Exp. Med.*, vol. 210, no. 12, pp. 2739–53, 2013, doi: 10.1084/jem.20130323.

[54] F. A. Scheeren *et al.*, "STAT5 regulates the self-renewal capacity and differentiation of human memory B cells and controls Bcl-6 expression," *Nat. Immunol.*, vol. 6, no. 3, pp. 303–313, 2005, doi: 10.1038/ni1172.

[55] S. A. Diehl *et al.*, "STAT3-mediated up-regulation of BLIMP1 Is coordinated with BCL6 down-regulation to control human plasma cell differentiation.," *J. Immunol.*, vol. 180, no. 7, pp. 4805–15, Apr. 2008, Accessed: Mar. 28, 2017. [Online]. Available: http://www.ncbi.nlm.nih.gov/pubmed/18354204.

[56] L. M. Heltemes-Harris and M. A. Farrar, "The role of STAT5 in lymphocyte development and transformation," *Current Opinion in Immunology*, vol. 24, no. 2. NIH Public Access, pp. 146–152, Apr. 2012, doi: 10.1016/j.coi.2012.01.015.

[57] K. Basso and R. Dalla-Favera, "Roles of BCL6 in normal and transformed germinal center B cells," *Immunol. Rev.*, vol. 247, no. 1, pp. 172–183, May 2012, doi: 10.1111/j.1600-065X.2012.01112.x.

[58] W. Luo, F. Weisel, and M. J. Shlomchik, "B Cell Receptor and CD40 Signaling Are Rewired for Synergistic Induction of the c-Myc Transcription Factor in Germinal Center B Cells," *Immunity*, vol. 48, no. 2, pp. 313-326.e5, 2018, doi: 10.1016/j.immuni.2018.01.008.